Online ISSN: 2981-0396 Print ISSN: 2981-0388

International Journal of Iron & Steel Society of Iran

Journal Homepage: https://journal.issiran.com/

Research Article

Analysis of a Six-Strand Continuous Casting Tundish for Billet Production with Implementating a Longitudinal Flow Control Tundish Dam

M. Salehi *[1], H. Soltani [2], M. Ehsani [3], A. Honarvar [4]

Mechanical Engineering Group, Department of Engineering, South Kaveh Steel Co, Bandar Abbas, Iran

ARTICLE INFO

Keywords:

Continuous Casting, Tundish, Numerical Simulation, Flow Control Tundish Dam, Molten Steel Flow.

Article history:

Received 28 August 2025
Received in revised form 10 November 2025
Accepted 05 May 2026

ABSTRACT

Proper tundish design plays a vital role in improving the metallurgical quality of the final product in the continuous casting process of steel. Key design objectives include increasing the residence time (RTD) of molten steel, reducing dead volume, and preventing the formation of direct flow paths. These factors promote the effective separation of impurities through argon gas injection and their flotation to the slag layer, ultimately enhancing product quality. In this study, the effect of implementing a longitudinal flow-control dam on the flow pattern inside a six-strand tundish is numerically investigated. Computational Fluid Dynamics (CFD) simulations are used to compare flow behavior with and without the dam. The results indicated that the dam significantly reduces dead volume, improves outlet flow uniformity, and enhances residence time. The model was validated using data from an industrial billet casting unit, confirming the practical feasibility of the approach.

1. Introduction

In the continuous casting process of steel, the tundish is a crucial component of the molten steel transfer system between the ladle and casting molds, playing a key role in controlling final product quality [1, 3]. While the early function of tundishes was limited to directing molten steel flow and ensuring continuous casting, the growing demand for higher metallurgical quality has transformed the tundish into a metallurgical reactor.

Modern tundishes are expected to perform several critical tasks, such as removing non-metallic inclusions, homogenizing chemical composition, reducing thermal fluctuations, and regulating flow profiles [4, 10]. Among these, the efficiency of inclusion removal is closely related to the tundish's internal hydrodynamic behavior. Key indicators used to assess tundish performance include the residence time distribution (RTD), dead zone volume, and plug-flow fraction. These factors determine how long molten steel remains inside the tundish and how much time is available for flotation and refining reactions to occur. Considering the importance of the contact between the molten steel surface and the injected gas bubbles in the tundish for promoting flotation and transferring inclusions to the slag layer, it is necessary to increase the residence time of the tundish.

To optimize flow conditions and enhance metallurgical performance, various design modifications have been proposed in recent years—particularly through the use of flow-control devices such as turbulence inhibitors and baffles. In 1999, Heaslip et al. [11] demonstrated that flow modifiers can effectively influence jet breakup and vortex

* *Corresponding Author*
Email: m.salehi@sksco.ir
Address: Mechanical Engineering Group, Department of Engineering, South Kaveh Steel Co, Bandar Abbas, Iran
1. M.S.c, 2. M.S.c, 3. M.S.c , 4. M.S.c

DOI: http://10.22034/IJISSI.2026.2070175.1327
Published by ISSI (Iron & Steel Society of Iran)

dynamics within the tundish. Later, in 2019, Delgado Ramirez et al. [12] showed that appropriately designed baffles can significantly enhance the hydrodynamic behavior of multi-strand tundishes, facilitating improved inclusion removal.

Additionally, the use of ladle shrouds as flow-controlling tools gained popularity between 2019 and 2023, contributing to performance improvements across different tundish configurations [13, 17].

Most previous studies have focused on improving inclusion removal by using argon gas injection or traditional transverse baffle designs. In this work, a new approach is proposed to optimize molten steel flow in the tundish. For the first time, a longitudinal dam tundish is applied in a six-strand billet casting tundish. This design helps to control the flow pattern, increase the effective residence time, and reduce dead zones. These factors play an essential role in inclusion flotation and improving steel cleanliness. The proposed design offers a simple, practical way to improve tundish flow behavior in multi-strand continuous casting.

This study aims to investigate the internal flow field of a six-strand billet-casting tundish and evaluate the impact of incorporating a longitudinal flow-control dam. Due to the difficulty of directly visualizing molten steel behavior, the flow analysis was performed using Computational Fluid Dynamics (CFD). Parameters such as velocity fields, residence time distribution, dead zones, and plug flow paths were evaluated.

The industrial data were obtained from the continuous casting unit of Kaveh South Steel Company, and the baseline numerical model (without the dam) was validated against experimental measurements. The results suggest that using a longitudinal flow-control dam effectively reduces dead zones and short-circuit flows, thereby promoting better energy distribution and enhanced steel cleanliness.

2. Research Methodology

2.1. Problem Definition

This study investigates the flow behavior of molten steel in two configurations of a six-strand continuous casting tundish. The first configuration corresponds to an industrial tundish with a 32-ton capacity, currently operating in the billet casting line of Kaveh South Kish Steel Company. The second configuration is a modified version of the same tundish geometry, incorporating a longitudinal flow control dam while maintaining identical dimensions. The dam is half the molten steel level and is designed to alter the internal flow field and improve hydrodynamic performance. Numerical analysis was performed using Computational Fluid Dynamics (CFD) simulations for both configurations.

2.2. Tundish Geometry

As illustrated in Fig. 1., the 3D geometry and dimensional model of the tundish were created using Autodesk Inventor. The left-hand image shows the original tundish design. In contrast, the right-hand image shows the modified version with the implemented longitudinal flow-control dam used for molten steel flow analysis.

2.3. Meshing

Due to the geometric symmetry of the tundish, only half of the domain was modeled in Fig. 2. to reduce computational costs and simulation time, without compromising accuracy. A mesh independence study was conducted using four different mesh sizes. As summarized in Table 1., a mesh containing approximately 4.73 million cells provided sufficiently converged results. The velocity and temperature contours in denser meshes exhibited negligible differences, confirming that the chosen mesh resolution was appropriate.

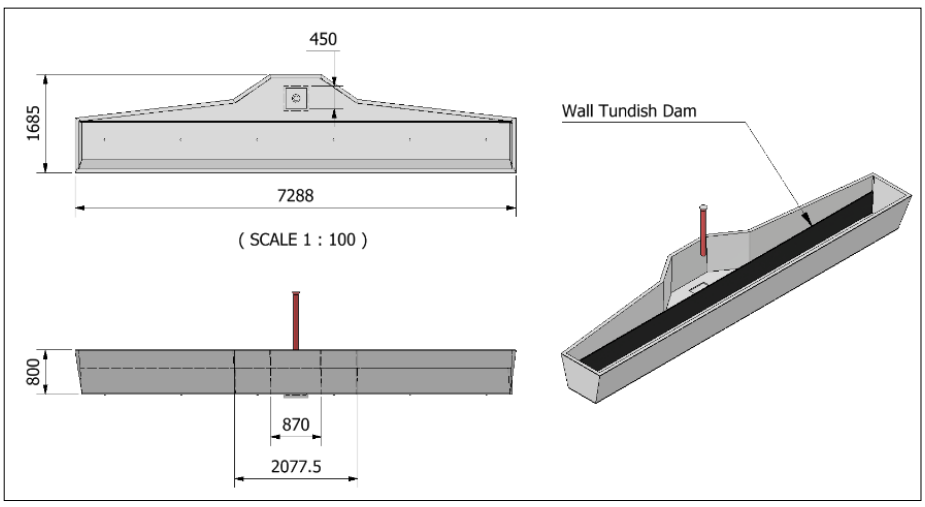

Fig. 1. Geometric dimensions of the six-strand billet tundish under study.

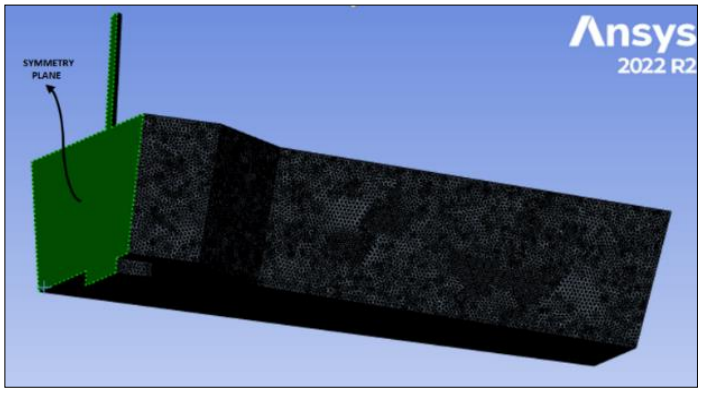

Fig. 2. Symmetrical geometry of the studied tundish.

Table 1. Mesh validation of the tundish model.

Cells	Mesh size (mm)	Outlet temperature (k)	Speed at outlet (m/s)
40735	100	1815.255	2.428
166660	75	1816.047	2.311
2538181	45	1816.871	2.124
4733011	25	1817.298	2.123

2.4. Governing Equations

The governing equations used in the simulation include:

Continuity Equation (Mass Conservation):

$$\frac{\partial \rho}{\partial t} + \frac{\partial(\rho v)}{\partial x} = 0 \qquad \text{Eq.(1)}$$

Momentum Equation:

$$\frac{\partial(\rho v_i)}{\partial t} + \frac{\partial}{\partial x_j}(\rho v_j v_i) = -\frac{\partial \rho}{\partial x_i} + \frac{\partial \rho}{\partial x_j}\left(\mu \frac{\partial v_i}{\partial x_j}\right) - \rho g_x \cdot \delta_{i1} + S_{V,i} \qquad \text{Eq.(2)}$$

The standard k-ε model was used to simulate turbulent flow, incorporating transport equations for turbulent kinetic energy (k) and its dissipation rate (ε).

Turbulent kinetic energy (k)

$$\frac{\partial(\rho k)}{\partial t} + \frac{\partial(\rho v_i k)}{\partial x_i} = \frac{\partial}{\partial x_j}\left|(\mu + \frac{\mu_t}{\sigma_k})\frac{\partial k}{\partial x_j}\right| + G_k + \rho\varepsilon \qquad \text{Eq.(3)}$$

Dissipation rate (ε):

$$\frac{\partial(\rho\varepsilon)}{\partial t} + \rho\frac{\partial(\rho\varepsilon v_i)}{\partial x_i} = \frac{\partial}{\partial x_j}\left|\left(\mu + \frac{\mu_t}{\sigma_k}\right)\frac{\partial \varepsilon}{\partial x_j}\right| + C_{1\varepsilon}\frac{\varepsilon}{K}G_k + C_{2\varepsilon}\frac{\varepsilon^2}{K} \qquad \text{Eq.(4)}$$

Where GK and μ_t are as follows.

$$G_k = \mu_t \frac{\partial v_j}{\partial x_i}\left(\frac{\partial v_i}{\partial x_j} + \frac{\partial v_j}{\partial x_i}\right) \qquad \text{Eq.(5)}$$

$$\mu_t = \rho C_u \frac{k^2}{\varepsilon} \qquad \text{Eq.(6)}$$

Where the values of C1ε, C2ε, Cμ, σk, σε are 1.44, 1.92, 0.09, 1.0, 1.3, respectively [21].

RTD and Flow Quantification Method

The average dimensionless concentration $\bar{C}$ of individual strand i (i = 6) can be expressed as:

$$\bar{C} = \frac{1}{n}\sum_{i=1}^{n} C_i \qquad \text{Eq.(7)}$$

The following equations can express the mean residence time t:

$$\bar{t} = \frac{\int_0^\infty \bar{c}tdt}{\int_0^\infty \bar{c}dt} \quad \text{Eq.(8)}$$

The dead volume fraction is calculated by:

$$V_d = 1 - \frac{\bar{t}}{t_0} \quad \text{Eq.(9)}$$

where t_0 means the theoretical residence time, which is considered as:

$$t_0 = \frac{V_{model-tundish}}{V_{outflow-rate}} \quad \text{Eq.(10)}$$

The consistency is defined by the overall standard deviation of RTD curves, which can be calculated by:

$$s = \frac{1}{N}\sum_{j=1}^{N}\sqrt{\frac{\sum_{i=1}^{n}[E_i(\theta_j)]^2}{n}} \quad \text{Eq.(11)}$$

where N is the amount of measured data; $E_i(\theta_j)$ presents the dimensionless concentration of the ith stream at moment j; $E(\theta j)$ denotes the average dimensionless concentration at moment j; and n is the number of strands.

2.5. Boundary Conditions

The molten steel inside the tundish was modeled as a single-phase, incompressible, and turbulent fluid. The standard k-ε turbulence model was employed due to its proven accuracy and widespread application in steelmaking CFD simulations [18–20].

The boundary conditions applied in this study were as follows:

Inlet: The inlet boundary was defined with a constant temperature of 1823 K and a specified mass flow rate of 2.16 kg/s (equivalent to 3 tons/min). The inlet velocity profile was fully developed.

Outlet: The tundish outlets were modeled as outflow boundaries, allowing the fluid to exit freely without any back pressure or turbulence specification.

Top Surface: The top surface of the molten steel was assumed to be a free surface with zero shear stress, i.e., no momentum exchange with the environment.

Symmetry Plane: Due to the geometric symmetry of the tundish, a symmetry boundary condition was applied at the longitudinal mid-plane. The gradient of all variables normal to the symmetry plane was set to zero.

Walls: All tundish walls were modeled with a no-slip boundary condition, implying zero velocity at the solid boundaries. A standard wall function was used to model the near-wall flow behavior, avoiding the need for an excessively fine mesh near the walls.

Heat Transfer: Heat loss was modeled through conduction and convection on the tundish surfaces:

Top Surface: The heat transfer coefficient was 15 W/m²·K, accounting for both convective and radiative losses.

Side walls and Bottom Surface: The heat transfer coefficient was 3.46 W/m²·K [9].

Thermal Conductivity of Molten Steel: The specific heat capacity was 640 J/kg·K.

Gravity: The gravitational acceleration was set to 9.81 m/s², directed downward.

Radiation and Slag Layer Effects: The effects of slag layer and radiation were neglected to simplify the model.

Solver Settings: The pressure-based solver was used, and the SIMPLEC algorithm was applied for pressure–velocity coupling. Convergence was considered achieved when residuals dropped below 10^{-4}.

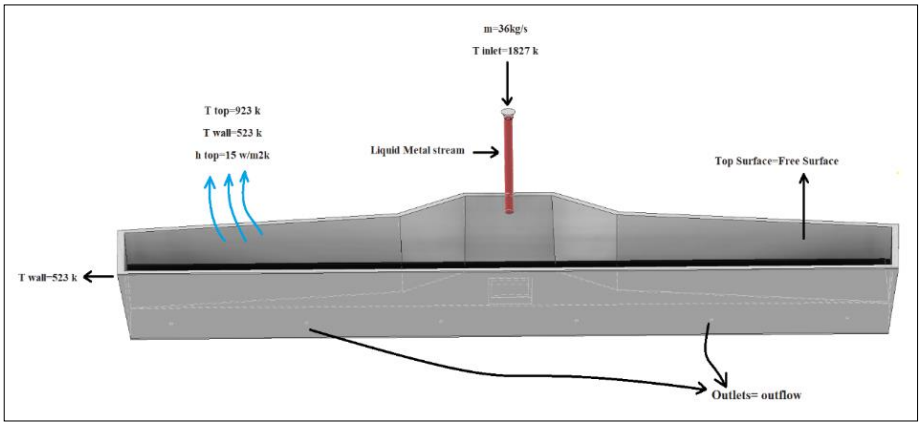

Fig. 3. Boundary conditions applied to the six-strand billet casting tundish.

Table 2. Geometric parameters and fluid properties.

Parameter	Unit	Value
Inlet flow temperature	[K]	1823
Top wall temperature	[K]	1200
Side wall temperature	[K]	523
Number of strands	[kg/m^3]	7200
Casting speed	[W/m k]	35
Mass flow rate	[J/kg·k]	640
Liquid steel and tracer density	[m]	0.018
Heat transfer coefficient (top surface)	[-]	6
Heat transfer coefficient (walls)	[m/min]	3
Thermal conductivity of molten steel	[Kg/s] [Ton/minute]	36 2.16
Specific heat capacity of molten steel	[W/m^{2}K]	15
Total molten steel volume	[W/m^{2}K]	3.46
Outlet nozzle diameter	[Metric Ton]	32
Shroud internal diameter	[m]	0.067

3. Esults and Discussion

Both qualitative and quantitative analyses were performed using CFD simulation results to evaluate the effect of the longitudinal flow-control dam on the molten steel flow characteristics. Velocity contours and vector fields were analyzed in horizontal and vertical cross-sections, providing insight into vortex formation, short-circuit flows, and dead zones.

3.1. Velocity Contours and Flow Distribution

Cross-sectional contours in Fig. 4. and top-view contours in Fig. 5. were analyzed to evaluate the effect of the flow control dam on the hydrodynamic behavior of molten steel in the tundish. These visualizations, together with velocity vector analysis, provide detailed insight into flow pattern variations, vortex intensity, shortcut flow paths, kinetic energy distribution, and the location of low-velocity zones.

As shown in Fig. 4., the initial impingement of the inlet jet on the dam causes the flow to deviate upward and toward the sides in the model with a flow control dam. This flow deflection suppresses direct penetration to the tundish bottom and consequently reduces the refractory wear rate. Additionally, the redistribution of kinetic energy stimulates flow in the side regions, thereby preventing the formation of dead zones. The dampening of the inlet velocity also increases the effective residence time and improves conditions for metallurgical reactions within the flow path.

In contrast, in the absence of a dam, the high-speed jet flows directly toward the tundish bottom, forming a shortcut path with minimal hydraulic resistance, significantly reducing the effective utilization of the tundish volume. In such cases, side zones remain hydrodynamically inactive, turning into low-velocity regions with poor mass and heat transfer characteristics.

Fig. 5. exhibits the vertical plane velocity contours. In the dam-equipped model, the redirected flow is more uniformly distributed across a wide area of the tundish. The velocity coloring indicates mid-range values across the upper surface of the molten steel, thereby reducing thermal and chemical fluctuations at the outlets. In the no-dam model, high fluid velocity is concentrated around the ladle shroud, with sharp flow intensity in that region. In contrast, along the longitudinal walls and in the rear region of the tundish, near-zero-velocity zones appear, indicating weak transverse mixing and the presence of horizontal-plane dead regions.

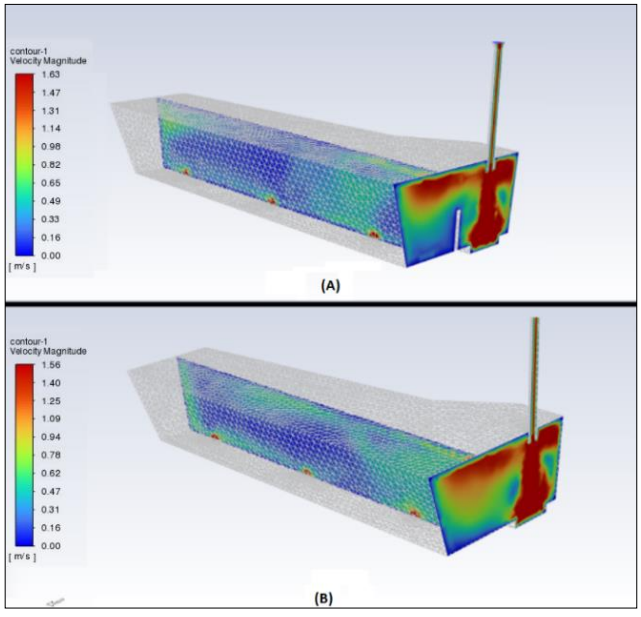

Fig. 4. Cross-sectional view of the velocity contours: (A) tundish with flow control dam; (B) tundish without dam.

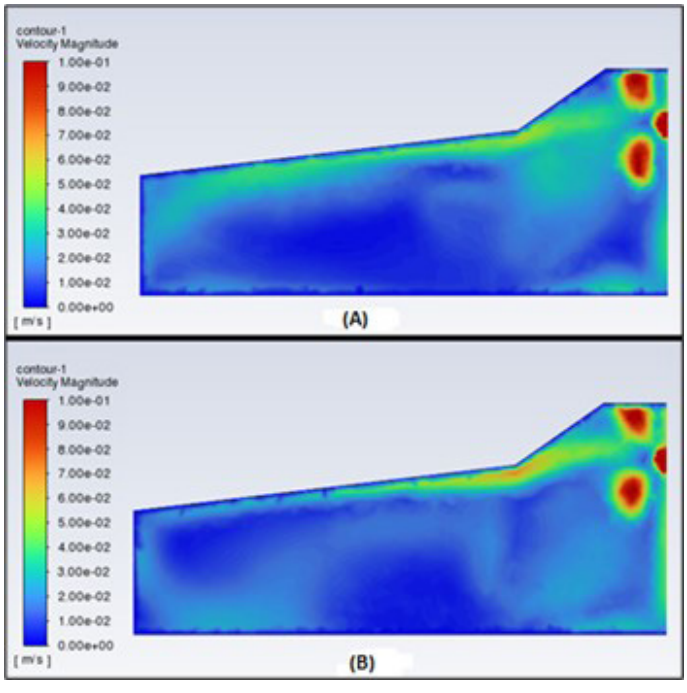

Fig. 5. Top view of velocity contours: (A) tundish with flow control dam; (B) tundish without dam.

3.2. Velocity Vector Analysis

Fig. 6. illustrates velocity vectors in a longitudinal section across the outlets. Subfigure (a) represents the tundish with the dam, and (b) shows the tundish without it. These images clearly demonstrate the dam's role in controlling the flow field, minimizing dead zones, and improving the rotational behavior of the flow. In the no-dam condition, the incoming jet flows almost directly through the tundish, forming two large vortices near the inlet and outlet zones. This type of flow concentrates velocity along the tundish centerline, while the central region remains relatively inactive. The formed vortices are free and unstable, contributing to the development of dead volume.

In contrast, the addition of a flow-control dam significantly alters the flow structure. The dam breaks the incoming jet and reinforces controlled rotational flow within the tundish core. The resulting flow becomes more symmetric, with more stable vortices throughout the

molten volume, increasing the mixing rate and effective residence time. Moreover, velocity vectors around the outlets are oriented to reduce direct shortcut flow paths, increasing the opportunity for inclusion flotation and slag removal. In summary, Fig. 6. demonstrates that using a flow control dam, by redirecting flow into structured rotational paths, enhances hydrodynamic performance and significantly reduces inactive zones in the tundish.

Fig. 7. presents top-view velocity vectors in which subfigure (a) corresponds to the tundish with a flow dam, and (b) shows the tundish without it. As illustrated, the flow patterns in the two geometries differ significantly. In the no-dam configuration, the inlet jet from the ladle shroud strikes the opposite wall at high velocity and then forms two dominant vortices that redistribute toward the outlets. This behavior causes velocity concentration along a direct path and increases the likelihood of molten steel shortcutting to the outlet. It also limits lateral mixing and leads to low-velocity zones in the corners and near the outlets, forming a considerable volume of dead space near the bottom and sidewalls of the tundish.

In contrast, in the tundish with a flow dam, the incoming flow enters the interior in a more controlled manner. The dam breaks the incoming jet, redistributes kinetic energy, and strengthens rotational motion in the tundish core. As a result, the velocity vectors are more symmetrically distributed, and targeted vortices form near the inlet and central zones. This phenomenon reduces shortcut velocities and increases transverse mixing and suppresses dead zones, improving the uniformity of the flow field. Based on the color range and vector scale, although peak local velocity is lower, the intensity and direction of the flow in the dam-equipped case are more balanced and controlled. This leads to longer residence time, improved inclusion flotation, and more homogeneous thermal and chemical conditions in the molten steel.

3.3. Thermal Distribution Analysis

Fig. 8. presents the variations in molten steel temperature at the three tundish outlets for both cases. These graphs were analyzed to evaluate thermal uniformity of the tundish outlets as an essential factor for final product quality and avoiding thermal instability in continuous casting.

In the no-dam configuration, there is a noticeable temperature difference of about 2 K among the three outlets, with the first nozzle being hotter than the other two. This imbalance results from the direct, rapid transfer of molten steel from the inlet to the nearest outlet, while dead zones form along the flow path to the

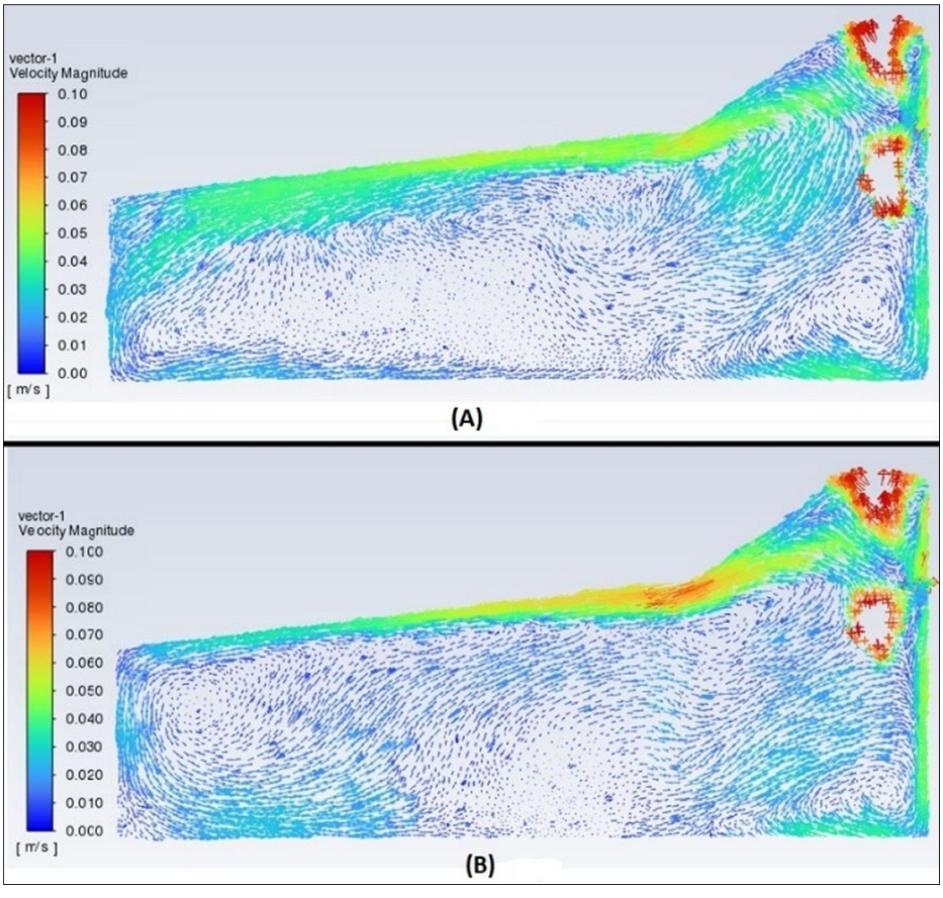

Fig. 6. Longitudinal velocity vectors along the outlets: (A) tundish with flow control dam; (B) tundish without dam.

more distant outlets. Such a heterogeneous temperature distribution can cause thermal instability and reduce the surface quality of billets at different strand positions.

In contrast to the dam, the flow becomes more uniform, and the temperature at all outlets stabilizes at 1816 K, ensuring better process stability and casting quality. This improved thermal uniformity is a direct outcome of the dam's role in redistributing kinetic energy, enhancing lateral mixing, and reducing stagnant zones. In other words, the flow control dam, by controlling the direction and intensity of the incoming jet, creates more uniform thermal conditions throughout the tundish, which is critical for maintaining process stability and consistent casting quality.

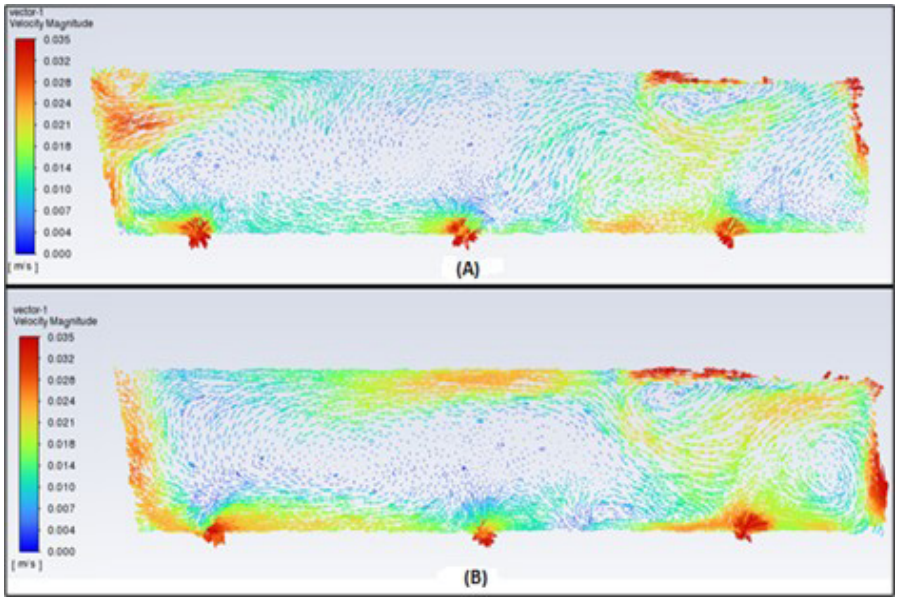

Fig. 7. Top view of velocity vectors: (A) tundish with flow control dam; (B) tundish without dam.

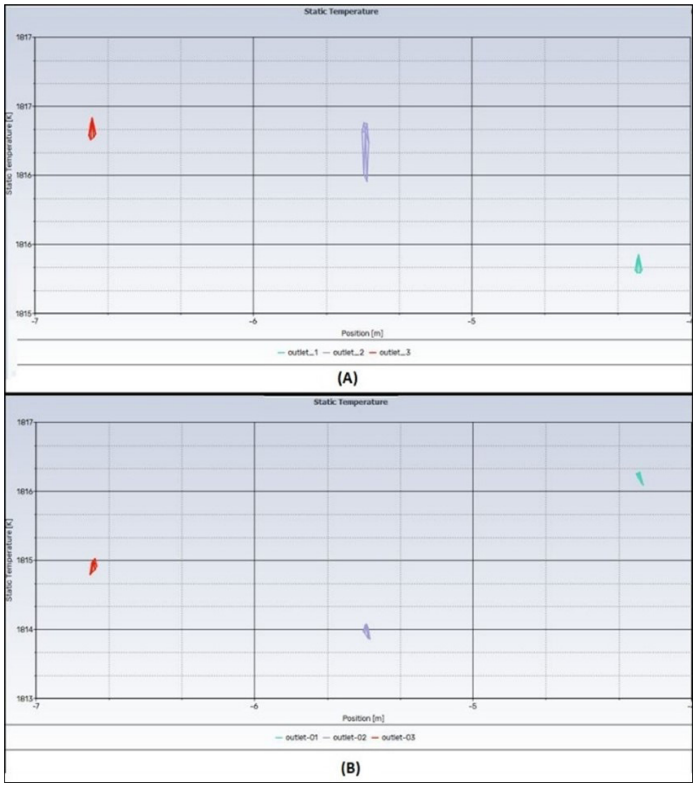

Fig. 8. Comparison of temperature distribution at the three outlets: (a) tundish with flow control dam; (b) tundish without flow control dam.

4. Conclusions

In this study, the hydrodynamic and thermal performance of a six-strand billet continuous casting tundish was investigated using computational fluid dynamics (CFD) to evaluate the effects of introducing a longitudinal flow-control dam. The numerical results confirmed that installing the dam significantly altered the internal flow structure, breaking the inlet jet and generating stable, symmetric recirculation zones. This modification increased the effective residence time, reduced shortcut flow paths, and enhanced mixing efficiency within the tundish. Moreover, the dam led to a more uniform distribution of kinetic energy, minimized dead zones, and improved plug flow characteristics. The temperature differences among the outlets were also reduced, resulting in better thermal homogeneity and improved casting stability.

The main findings of this work were:

- Increased residence time of molten steel inside the tundish.
- Improved symmetry and stability of flow circulation.
- Enhanced kinetic energy distribution and reduced dead volumes.
- Improved outlet temperature uniformity.
- Suppression of shortcut flow from inlet to outlet.

Overall, incorporating a longitudinal flow-control dam is a simple and cost-effective approach to enhance the flow field and metallurgical performance in billet-casting tundishes.

Nomenclature

Symbol	Explanation
ρ	fluid density (kg/m³)
$\vec{v}$	fluid velocity (m/s)
P	pressure (Pa)
μeff	effective viscosity
F	Force (N/m^3)
k	Turbulent kinetic energy (J/kg)
ε (epsilon)	Turbulent energy dissipation rate (m^2/s^3)
μ	Dynamic viscosity (Pa·s)
μt	Turbulent viscosity (Pa·s)
Gk	Turbulent kinetic energy generation term
xi	Spatial coordinate in direction i (i = 1,2,3) (m)

References

[1] Morales R, Lopez Ramirez S, Palafox Ramos J, Zacharias J, Numerical and modeling analysis of fluid flow and heat transfer of liquid steel in a tundish with different flow control devices, ISIJ Int. 1999; 39: 455-462.
[2] Jin Y, Dong X, Yang F, Cheng C, Wang W, Removal mechanism of microscale non metallic inclusions in a tundish with multi hole double baffles, Metals. 2018; 8: 611.
[3] Sahai Y, Tundish technology for casting clean steel: A review, Metall Mater Trans B. 2016; 47: 2095-2106.
[4] Mazumdar D, Guthrie R, The physical and mathematical modelling of continuous casting tundish systems, ISIJ Int. 1999; 39: 524-547.
[5] Sheng D, Mathematical modelling of multiphase flow and inclusion behavior in a single strand tundish, Metals. 2020; 10: 1213.
[6] Chattopadhyay K, Physical and Mathematical Modelling of Steelmaking Tundish Operations: A Review of the Last Decade (1999–2009), ISIJ Int. 2010; 50: 331-348.
[7] Mazumdar D, Review, analysis, and modeling of continuous casting tundish systems, Steel Res Int. 2019; 90: 1800279.
[8] Fang Q, Mazumdar D, Guthrie R, Optimization of flow, heat transfer and inclusion removal behaviors in an odd multistrand bloom casting tundish, J Mater Res Technol. 2020; 9: 347-363.
[9] Tang H, Improved Metallurgical Effect of Tundish through a Novel Induction Heating Channel for Multistrand Casting, Metals. 2021; 11: 1075.
[10] Yang B, Power curve key factor affecting metallurgical effects of an induction heating tundish, J Iron Steel Res Int. 2022; 29: 151-164.
[11] Heaslip L.J, Physical modeling and visualization of liquid steel flow behavior during continuous casting, Iron Steelmaker. 1999; 26: 33-41.
[12] Ramirez O.S.D, Thermal and Fluid Dynamic Optimization of a Five Strand Asymmetric Delta Shaped Billet Caster Tundish, Steel Res Int. 2018; 89: 1700428.
[13] Zhang J, Advances in ladle shroud as a functional device in tundish metallurgy: A review, ISIJ Int. 2019; 59: 1167-1177.
[14] Zhang H, Multiphase Flow in a Five Strand Tundish Using Trumpet Ladle Shroud during Steady State Casting and Ladle Change Over, Steel Res Int. 2019; 90: 1800497.
[15] Yang L, On the Ladle Shroud Design and Mis alignment Effects on the Fluid Flow in a Metallurgical Tundish – A CFD Model Study, E3S Web Conf. 2020; 185: 04069.
[16] Zhang J, Comparison of Multiphase Flow in a Continuous Casting Tundish Using Two Types of Industrialized Ladle Shrouds, JOM. 2018; 70: 2886-2892.
[17] Safaei H, Asadi B, The Effect of the Angle of Molten Metal Exit From the Submerged Nozzle on the Flow Inside the Casting Mold, ISSI (Iron & Steel Society of Iran). 2025; 22(1): 1-8.
[18] Yang B, Exploration of the Relationship between the Electromagnetic Field and the Hydrodynamic Phenomenon in a Channel Type Induction Heating Tundish Using a Validated Model, ISIJ Int. 2022; 62: 677-688.

[19] Chang S, Simulation of Flow and Heat Fields in a Seven strand Tundish with Gas Curtain for Molten Steel Continuous Casting, ISIJ Int. 2015; 55: 837-844.
[20] Yang B, Numerical Study on the Influence of Distributing Chamber Volume on Metallurgical Effects in Two Strand Induction Heating Tundish, Metals. 2022; 12: 509.
[21] Launder B.E, Spalding D.B, The numerical computation of turbulent flows. In: Numerical Prediction of Flow, Heat Transfer, Turbulence and Combustion, Amsterdam (NL): Elsevier. 1983: 96-116.